2005

Microbubble-Based Model Analysis of Liquid Breakdown Initiation by a Submicrosecond Pulse

J. Qian
Old Dominion University

R. P. Joshi
Old Dominion University, rjoshi@odu.edu

K. H. Schoenbach
Old Dominion University

J. Dickens

A. Neuber

See next page for additional authors

Original Publication Citation

Qian, J., Joshi, R. P., Kolb, J., Schoenbach, K. H., Dickens, J., Neuber, A., . . . Gaudet, J. (2005). Microbubble-based model analysis of liquid breakdown initiation by a submicrosecond pulse. *Journal of Applied Physics, 97*(11), 113304. doi:10.1063/1.1921338

Microbubble-based model analysis of liquid breakdown initiation by a submicrosecond pulse

J. Qian, R. P. Joshi,[a] J. Kolb, and K. H. Schoenbach
Department of Electrical and Computer Engineering, Old Dominion University, Norfolk, Virginia 23529-0246

J. Dickens, A. Neuber, M. Butcher, M. Cevallos, and H. Krompholz
Department of Electrical and Computer Engineering, Texas Tech University, Lubbock, Texas 79409-3102

E. Schamiloglu and J. Gaudet
Department of Electrical and Computer Engineering, University of New Mexico, Albuquerque, New Mexico 87131

(Received 10 January 2005; accepted 29 March 2005; published online 31 May 2005)

An electrical breakdown model for liquids in response to a submicrosecond (~100 ns) voltage pulse is presented, and quantitative evaluations carried out. It is proposed that breakdown is initiated by field emission at the interface of pre-existing microbubbles. Impact ionization within the microbubble gas then contributes to plasma development, with cathode injection having a delayed and secondary role. Continuous field emission at the streamer tip contributes to filament growth and propagation. This model can adequately explain almost all of the experimentally observed features, including dendritic structures and fluctuations in the prebreakdown current. Two-dimensional, time-dependent simulations have been carried out based on a continuum model for water, though the results are quite general. Monte Carlo simulations provide the relevant transport parameters for our model. Our quantitative predictions match the available data quite well, including the breakdown delay times and observed optical emission. © *2005 American Institute of Physics*. [DOI: 10.1063/1.1921338]

I. INTRODUCTION

There is considerable interest[1–8] in the study of electrical breakdown in water (and other liquids) for pulsed power systems, for their use in energy storage, towards insulation of high-voltage devices, in acoustic devices, and as the medium in spark erosion machines. Liquids seem to have advantages over gases and solids for both energy storage and as switch media, particularly for nanosecond pulse generators. For example, liquids not only have a high dielectric constant, but also have higher breakdown strength than compressed gases.[7] Water has been used and found to hold off electrical fields of about 2 MV/cm for durations up to hundreds of nanoseconds.[9,10] In comparison to solids, their ability to circulate leads to better thermal management and easier removal of debris after breakdown. Liquid dielectrics are also better suited for applications involving complex geometries.

The electrical behavior of dielectric liquids (especially water) subjected to high electric fields has been intensively studied.[11–20] Despite the progress, there is as yet no final and complete understanding of issues relating to the initiation process, the physics of charge creation in liquids, and the subsequent plasma dynamics (e.g., the observed fast-moving streamers) on the submicrosecond time scales. Potential mechanisms for plasma generation within the liquid include impact ionization, field-assisted emission (i.e., Zener tunneling), or a combination of both. However, the former not only requires the presence of seed electrons, but also that some particles from this population have energies exceeding the ionization threshold. As we discuss here, it is difficult to attain mobile electrons in liquids and even more arduous to impart the requisite high energies for impact ionization despite the application of large electric fields. Zener tunneling requires very large electric fields. Hence, it is not very likely to occur naturally and easily at the electrode-liquid interfaces, or within the bulk liquid. However, localized enhancements in electric field, either through asperities at the metallic contacts or due to the presence of microscopic bubbles in the bulk liquid, could boost this mechanism.

Two competing theories of liquid breakdown have been discussed in the literature: (i) A bubble-initiated breakdown process and (ii) an electronic impact-ionization process within the bulk liquid. The proposed electron-initiated mechanism in bulk liquid does not appear to be very plausible for several reasons. (i) First, electron avalanche processes in the bulk liquid are nearly negligible.[11] As our own calculations have shown recently,[21] relatively high scattering cross sections coupled with the largely isotropic elastic scattering excludes the possibility for electrons in bulk water to acquire significant kinetic energy for impact ionization. The electrons are most likely to undergo a large number of random scattering events (i.e., exhibit a very short mean free path) and quickly attach to neutral molecules to form "electron bubbles,"[22,23] or recombine with positive ions. (ii) Second, free electrons are generally absent in water since an enormous increase in entropy is required to convert an electron into a negative ion by attachment. This dearth of free electrons can alternatively be viewed as arising from the

[a]Electronic mail: rjoshi@odu.edu

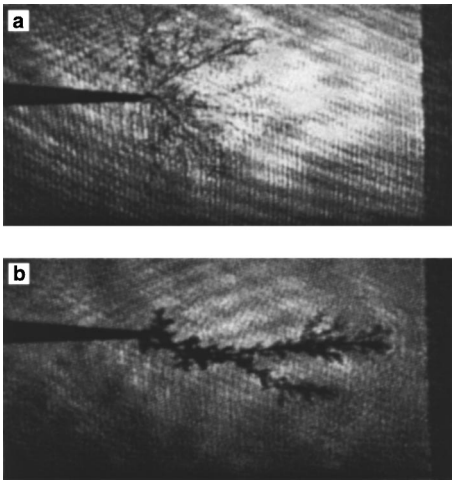

FIG. 1. Typically representative streamer in oil for a point-plane geometry. (a) Snapshot for a positively biased point contact and (b) snapshot for a negatively biased point electrode.

large "band gap" of water, which is ~8.5 eV,[24] and the high barrier height between the metal-liquid interface. Furthermore, recent experimental data clearly show that free electrons are quickly solvated within ~1-ps time scales.[25] Hence, the probability for a free electron population is likely to be negligible. (iii) Finally, the observed dependence of breakdown on hydrostatic pressure and voltage pulse duration points towards the role of gas/vapor bubbles. For example, a high hydrostatic pressure would either inhibit bubble formation or shrink their size, resulting in an observed increase of the hold-off strength.[26] Similarly, since longer pulses allow more time for bubble nucleation or increases in size through internal heating and Maxwell stress-related deformation, such long pulses lead to decreases in the required breakdown field.

It is perhaps useful to review some of the salient features observed during liquid breakdown. The following set of experimental observations has been reported in the literature, and is fairly universal. (i) A distinct polarity effect is seen for point-plane (or similarly asymmetric) geometries.[1,10,27,28] The breakdown voltage ($=V_{br}$) is universally observed to be *lower when the point electrode is biased positively*. Based on gas discharge physics, one might expect liquid water breakdown to be initiated at the cathode due to possible electronic injection. The experimental data, however, suggest otherwise, and instead indicate that mechanisms other than pure cathodic electron injection must be relevant to breakdown. (ii) Streamer formation and dynamics, during the breakdown process, have been seen to have different geometric shapes and velocities depending on the polarity of the pin electrode. The streamers originating on the positive electrode form earlier in time, they travel faster, and do not tend to exhibit velocity saturation with the electric field magnitude.[29] For example, streamers formed from the anode tip typically have more branches and a distinct "treelike" structure spanning a conical volume, as shown in Fig. 1(a). Cathode-tip streamers, on the other hand, are less bushy and usually have a prominently thick "root" structure as indicated in Fig. 1(b). (iii) Discrete optical luminosity spots have been seen on

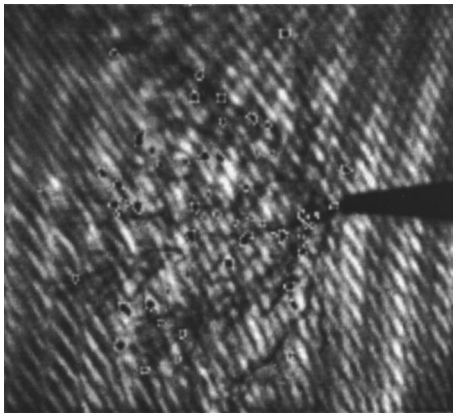

FIG. 2. Experimentally obtained luminosity spots at discrete locations on the streamer branches during a prebreakdown snapshot for oil.

streamer branches as shown in Fig. 2. Experimental details relating to this data of Fig. 2 have been reported elsewhere.[28] (iv) External pressure appears to affect the breakdown voltage. Increasing the overpressure typically tends to enhance the breakdown voltage, while underpressures have been observed to decrease the breakdown voltage. This suggests that microbubbles might have some role in the breakdown process. Some of the experimental data, shown in Fig. 3, demonstrate this more clearly. With decreasing pressure, the breakdown voltage is seen to reduce. (v) Electrical current spikes of a random nature are usually observed during the prebreakdown phase of liquid breakdown. Both polar solvents (such as water) and nonpolar liquids (such as oils) have reportedly exhibited such behavior. The pertinent data obtained by our group are shown in Fig. 4. The results are indicative of partial triggering or localized turn-on. Furthermore, such current spikes appear to correlate well with the number of luminous spots appearing within the liquid upon external voltage stressing. We postulate here that localized breakdown within microbubbles contributes to the current spikes and also to the observed optical luminescence within the microregions. (vi) Polishing the electrodes (especially the anode) appears to help enhance the hold-off voltage. Management of asperities and the associated local electric-field enhancements, therefore, is important.[10] Figure 5 shows experimental data for water in the point-plane geometry with a 200-μm gap. As seen from the plot, a much higher hold-off voltage can be attained on polishing the point electrode. (vii) The magnitude of the breakdown voltage for lower dielectric

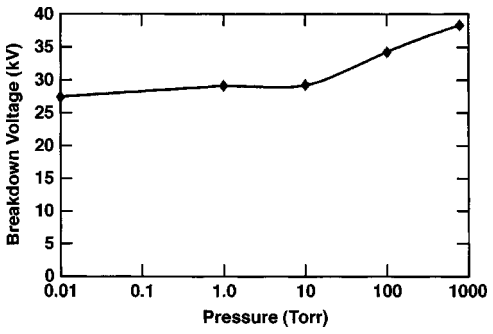

FIG. 3. Experimental data showing a pressure dependence of the breakdown voltage for oil.

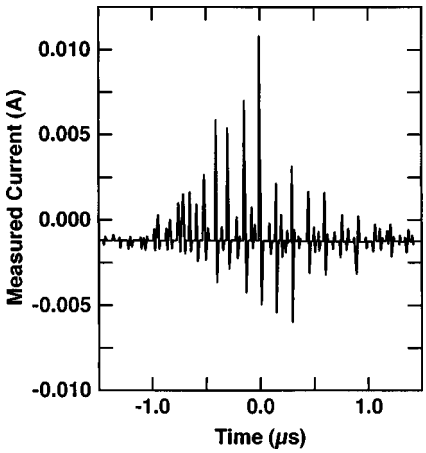

FIG. 4. Measured circuit current as a function of time in oil subjected to a voltage pulse.

liquids seems to be higher. For example, water (dielectric constant, $k_r \sim 80$) has been shown to break down at a field of about 1.8 MV/cm, while the corresponding field for propylene carbonate ($k_r \sim 65$) under otherwise identical conditions was observed to be 2.2 MV/cm. Oils (both biodegradable and transformer) with a much lower dielectric constant have been reported to have higher breakdown strengths. (viii) Finally, in a surprising result, the hold-off voltage for distilled water has been reported to be lower than that for ordinary tap water,[10] even though the prebreakdown current levels were higher. Since ion densities, and hence the conductivity of tap water, are larger, one might simply expect electrical breakdown to occur more easily in this system. We postulate that the observed behavior is a direct consequence of enhanced screening in tap water. The screening would work to shield the high electric fields and prevent them from penetrating into microbubbles that are likely to be located randomly within the bulk. Consequently, there would be greater likelihood of alleviating the bubble-initiated triggering mechanism in tap water as compared to distilled or pure water.

In our previous work based on a continuum model, it was shown that the energy associated with a submicrosecond pulse is too low to induce any significant heating. Temperature increases of less than 6 K were predicted[30] for such

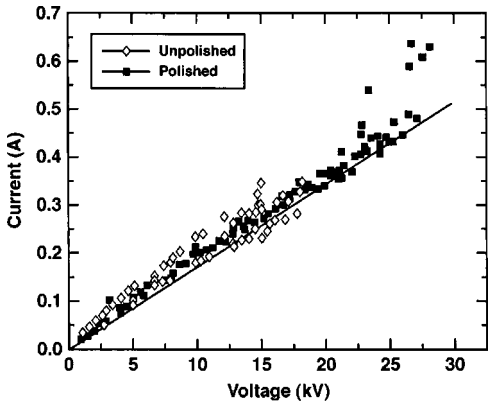

FIG. 5. Measured current–voltage data points for water for a 200-μm point-plane geometry showing differences between polished and unpolished electrode surfaces.

situations. Hence, bubble formation on the basis of localized liquid vaporization can effectively be ruled out. We have also demonstrated through Monte Carlo calculations that free-electron transport and possible electronic impact ionization in bulk water would be virtually absent.[21] The numerical analysis quantitatively demonstrated that strong elastic scattering coupled with the highly isotropic angular deflections work to prevent electrons from picking up the requisite ionization energy. As a result, neither electron-initiated charge creation within the homogeneous bulk nor the electronic injection process at the cathode can have much relevance for breakdown.

Here a general model of liquid breakdown is developed that incorporates two important features. First, the *preexistence of spatially localized microbubbles*, in equilibrium with the liquid phase, is implicitly assumed. As a result, no strong internal heating or vaporization is necessary for the creation of local low-density regions. Such bubbles are assumed to be filled with dissolved gas. Next, in keeping with experimental reports (as discussed, for example, in the case of water[25]), it is assumed that free electrons are generally absent in liquids. Instead, more realistically, the experimental observations indicate that free electrons have a short and finite lifetime before an attachment or recombination event takes place. Consequently, the likelihood of the electrons' survival can be expected to progressively decrease with increasing distance from their generation sites.

Quantitative calculations have been carried out here, that include the two above assumptions, to analyze the breakdown process. First, a Monte Carlo (MC) model has been applied to ascertain the relevant transport parameters such as the impact ionization and electron drift velocity. The field, spatial, and temporal dependencies are naturally included. The MC results are then used for a continuum drift-diffusion model of charge transport to obtain the time-dependent current and voltage behavior over submicrosecond time scales. It is demonstrated that this physical model can adequately explain most of the experimental observations. Though the model generally applies to all liquids, for concreteness here, calculations of the breakdown process have been performed for liquid water.

II. DISCUSSION OF THE BREAKDOWN MODEL

We postulate that liquid breakdown is initiated via the field-emission process within localized, low-density regions (i.e., microbubbles) upon being subjected to high electric fields. The possible existence of stable microscopic gas bubbles within liquids was proposed by Bunkin and Bunkin.[31] They referred to such entities as "bubbstons." The notion of invoking gas bubbles in liquids originally arose from a separate effort to explain the lower rupture strength of liquids.[32] Bunkin and Bunkin[31] studied the formation and stabilization dynamics, and concluded that bubbstons could exist in the presence of trace impurities (including ionogenic surface-active agents) and localized ions. Such microbubbles are likely to be randomly scattered throughout the bulk of the liquid volume and also be present at electrode surfaces.

Discontinuity in the dielectric constant between the sur-

rounding liquid and the interior of the bubble helps create electric-field enhancements on the gaseous side of the microbubble interface. The field within the cavity is uniform[33] and depends only on the external field (about 2 MV/cm in water near the breakdown phase) and the ratio of the liquid-gas permittivities. Smaller values of the liquid permittivity would lead to a lower electric field within the microbubble. This could produce a greater hold-off capability, in line with the higher breakdown voltages seen for propylene carbonate (a lower dielectric material) as compared to water. We postulate that electrons are injected into the gas bubble via the field-emission process at the bubble-liquid interface. Subsequent acceleration by the electric field within the bubble then leads to a strong energy gain and impact ionization of the bubble gas. Thus, *bubbles act as localized microsources of charge* and contribute to plasma creation and multiplication within the liquid.

The following effects should then arise due to the collective influences of a large electrostatic driving force on the electrons, the inherent scattering with gas molecules, and the subsequent impact ionization events.

(i) Sudden and discrete increases in the external current as individual bubbles develop into active microcenters of charge creation. Such current spikes, as predicted by the present model, have actually been observed experimentally. In time, however, the electric field within each microbubble would be expected to diminish as the result of charge-induced, intrabubble polarization. This would partially quench the current contribution from an individual "electrically activated" microbubble. The net result would be multiple, but sporadic, current spikes.

(ii) A second effect is the possible emission of radiation encompassing the microbubbles. A combination of processes, such as field-induced acceleration, Coulomb scattering of the charges, and radiative recombination would collectively contribute. Such localized pockets of radiation and optical emission have been observed, with the results of Fig. 2 being an illustrative example. Apart from frequency-dependent Bremsstrahlung, the emission spectra can also be expected to contain lines characteristic of gaseous excitation and absorption. In addition, radiative recombination of electrons (moving downstream towards the anode), with ions generated originally from a neighboring microbubble, would also be present.

(iii) The present model predicts an effect of both the external pressure and operating temperature on the breakdown voltage magnitude. With increasing external operating pressure, for example, the microbubble size would decrease. This would lead to a larger field requirement for producing a given amount of charge multiplication within the confined space. Similarly, increases in temperature could reduce the microbubble density due to their evaporation from the liquid phase. Consequently, the probability of a microbubble lying within a localized high-field region would diminish. This would lead to an overall increase in the requisite field or a longer delay time for breakdown. Such changes with pressure have been observed in our group, for example, as shown in Fig. 3. If, however, the bubble population remained stable despite temperature variations (for example, due to large fluid viscosity that prevented bubble movement and evaporation), then their size would change. This would alter the charge multiplication factor within the microbubble volume and again impact the breakdown field. However, for most liquids of practical interest, this is unlikely.

(iv) In the scenario described here, the breakdown process would likely initiate in a region of high electric field that promotes electron emission. This would most likely be on the gaseous side of a microbubble-liquid interface, and occur close to an electrode. Surface asperities and sharp curvatures would strongly facilitate this initiation. Hence, smoothening the electrodes should enhance the hold-off voltage capability. Furthermore, the presence of a strong ion density would work to mitigate the electric-field magnitude and arrest its penetration into the microbubble areas. As a result, an influence of ionic concentration on the breakdown threshold voltage can be expected.

(v) In this setting, microbubbles would continue to play a role in the temporal development of the breakdown process. For example, if multiple microbubbles were to be located along a straight-line path between the initial triggering point and the electrodes, then bifurcation of the plasma channel can be expected. Through the process of successive and sequential breakdown of microbubbles, the breakdown path might be expected to zigzag, hopping from one bubble to the next. Such branching or "treeing" structures have experimentally been observed by numerous groups. Another physical basis for the branching might arise from mutual electrostatic repulsion between high-density pockets of spatially nonuniform electrons within the moving streamer. Such a mechanism has recently been proposed in gases,[34] but remains to be investigated in liquids.

In our proposed model, streamer (or plasma) growth and propagation within the liquid primarily depends on the following factors. (i) The ionization rate within microbubbles, which is governed by the bubble radius and local electric field. This rate dictates plasma generation that then controls the dynamical collapse of the local electric field due to internal polarization effects. We propose that the collapse would trigger field increases across neighboring regions and microbubbles that, in turn, would initiate new, localized plasma generation events. Thus, the higher the ionization rate within microbubbles, the faster would be the conductive turn-on of localized segments within the overall liquid. (ii) The growth of the streamers would also depend on the magnitude and rate of energy dissipation by hot electrons emerging from the microbubbles. Electronic kinetic energies and effective temperatures are expected to be quite large due to strong electric field acceleration within the microbubbles. For example, a

ballistic electron under a 10^8-V/m field (the typical value close to the breakdown regime) within a 1-μm-diameter bubble would emerge with a 100-eV energy. Upon expulsion from the microbubble, such energetic electrons would convert their kinetic energy into heat through inelastic collisions with the water molecules, and thus impact-ionize localized regions. The net result could be large increases in local temperature and possible vaporization of small volumes adjacent to the microbubbles. The latter would cause a growth and elongation of the microbubble along the field direction. This process would primarily be operative for streamers initiating from the cathode side. Such dynamics could also possibly be relevant for anode-side streamer if a secondary microbubble were located close to the moving "anode-side" streamer head at some time instant. In this case, the high electric fields inside this secondary microbubble could trigger electron emission, and subsequently cause the electrons to turn on the intervening space between the advancing streamer head and the microbubble. Exact analysis of streamer growth based on such thermal conversion of electron energy requires Monte Carlo calculations as performed elsewhere for water by our group.[35] (iii) Continuous field-assisted electron emission from the streamer tip contributes to filamentary growth and propagation. This process would mainly be operative for anode-side streamers. (iv) A secondary effect is that of a possible electron injection from the cathode after filamentary structures have developed from the anode. For breakdown initiation from the anode side, the electric field in the anodic vicinity would gradually decrease, giving rise to field enhancements at the cathode neighborhood. Electronic-field emission from the cathode could then lead to the origination and growth of *secondary steamers* from the negative electrode. Such dual filamentary structures, with delayed cathode streamer formation and time-dependent propagation velocities, have recently been reported at Sandia National Laboratory.[29] Also, in such dual filament structures (with the initial breakdown occurring at the anode), the streamer propagation velocities would be high and increase dramatically in time after the development of the second streamer.

Next, the present model assumes that free electrons in the liquid have a short and finite lifetime, and that an attachment or recombination event must eventually take place. Thus, the likelihood of electron survival without capture should progressively decrease with increasing distance from their generation sites. Hence, electrons generated *close* to the anode (i.e., the parent microbubble lies close to the anode) would survive and contribute to current flow, regardless of their exact spatial origin. It then follows that streamers and optical emission patterns close to a point anode should exhibit a high degree of branching and tend to follow the divergent field lines. Also, the electric field would not have to be very large to provide a very high carrier drift to ensure efficient charge collection at the anode. On the other hand, for charge creation near the cathode (i.e., microbubbles located close to the negative electrode), the electron swarm would have a much longer transit region to traverse. For efficient and timely collection then, a much larger electric field would be needed to achieve a higher drift velocity for timely transit. The overall effect is an inherent asymmetry within the system that would work to create a polarity effect.

Based on the above discussion, the following general features should arise for point-plane geometries. (i) For electron creation near the cathode side, a *higher* electric field would be required to facilitate and ensure rapid transport of the electron swarm to the anode collector with transit times shorter than their lifetimes. (ii) The highest electric field occurs, in general, near a point electrode. Hence, if the point electrode were to be biased positively, then breakdown via electron emission and streamer growth would likely start at the anode. For a negatively biased point electrode, on the other hand, the breakdown could conceivably start at the cathode. However, there would be a finite chance of quenching the current if the emitted electrons did not survive their transit to the plane anode on the far side. So, the requisite voltage for attaining a complete breakdown would be higher for a negatively biased point. (iii) Finally, the luminescence and streamer patterns are predicted to be different for anode-side and cathode-side initiation. For a point anode case, several microbubbles in the vicinity of the sharp electrode would be triggered. Thus, a more pronounced treeing structure can be expected, aided by the divergent electric-field profile, and has been observed experimentally. For the case of point-cathode initiation, on the other hand, the growth and propagation are likely to have a strong contribution from hot-electron-assisted liquid vaporization and a process of "burrowing" into the liquid. Furthermore, the electric field between the streamer tip and the planar anode on the far side would be *less divergent*. Hence, the streamers and optical patterns are more likely to exhibit much smaller branching and have thicker roots. This general prediction is in keeping with the observations shown in Fig. 1.

III. THE MONTE CARLO MODEL FOR LIQUID WATER

We have previously reported on our three-dimensional, time-dependent Monte Carlo analyses of electron transport in liquid water.[35] The MC scheme is used here to furnish the relevant transport parameters for a continuum model based on the drift-diffusion scheme. Basically, electrons in liquid water undergo energy-dependent scattering that can be either elastic, inelastic ionization, or inelastic excitation.[36] The latter includes transitions towards the Rydberg or degenerate states, attachment leading to negative-ion generation, vibrational and rotational excitation, and excitation of the OH^*, H^*, and O^* radicals. In our analysis, the energy-dependent cross sections were parametrized based on a recent data report,[36] and discussed in detail previously.[35]

Monte Carlo simulations were carried out by injecting a swarm of 8000 particles into the microbubble at the gas-liquid interface for a given electric field. As a result, characteristics of the electron dynamics through the gas bubble, followed by their traversal in water, were obtained. Electron scattering within the bubble was implemented based on cross sections reported in the literature.[37–39] The initial energies were assigned based on a thermalized Boltzmann distribution. A time step of 0.01 fs was used for the highest water density (i.e., 1 gm/cc) because of the high elastic scattering rate shown in Fig. 6. The angular distribution was taken to be

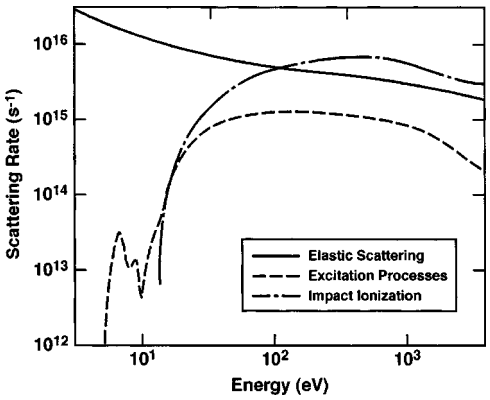

FIG. 6. Energy-dependent elastic and inelastic scattering rates used for the electron Monte Carlo in water.

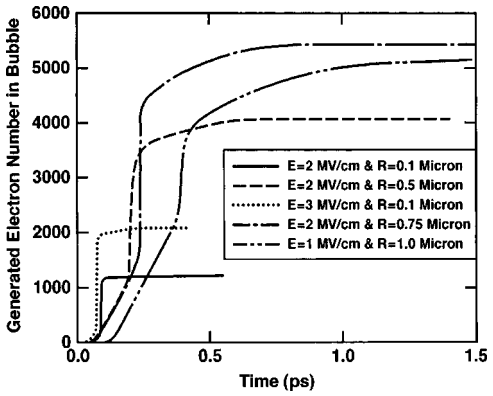

FIG. 8. Monte Carlo results showing secondary particle generation inside a bubble as a function of time due to an initial 8000-particle swarm.

isotropic for the inelastic processes. For elastic scattering, a Rutherford–Moliere[36] differential cross section was used.

Figure 7 shows time-dependent populations for swarms of 8000 electrons released simultaneously from one end of the bubble-water interface. Various cases for different bubble radii R and applied electric fields F are shown. All the curves of Fig. 7 exhibit a similar trend. An initial time delay is apparent in all cases—this is the "dead time" during which the electrons are within the bubble region and are picking up the requisite energy for impact ionization. The swarm then begins to produce secondary particles through the impact ionization process, and the overall population increases. This time delay naturally depends on the electric field and the bubble radius.

Strong increases in electron population roughly begin to occur when the swarm reaches the opposite end of the bubble and begins to enter the water. The high density within the liquid works to increase the scattering rate, and a sudden onset of ionization follows. In our simulation, particles in the water with energies below the ionization thresholds are removed from consideration, as essentially having thermalized. The time-dependent ionization replicas seen in Fig. 7 arise from a cyclical effect. First, low-energy particles from the swarm continually pick up energy from the electric field, reach the ionization threshold, and then fall back into lower energy states upon impact ionization.

Monte Carlo results for the time-dependent secondary particle production both inside and outside the bubble are given in Figs. 8 and 9. The values depend on the bubble radius and external electric field, with initial delay times in the subpicosecond regime. For the 8000 electron swarms, multiplicative gain factors of about 0.625 (=5000/8000) and 62.5 (=500 000/8000) are predicted inside and outside the bubble region, respectively. Furthermore, the number of electrons produced *outside the bubble is always more* than the secondary particles created within the bubble. This arises from the higher density in the liquid phase, and hence a larger collision rate for the high-energy electrons.

IV. TIME-DEPENDENT RESULTS FOR LIQUID WATER

A time-dependent, two-dimensional simulation model as reported and discussed elsewhere,[21] was used for numerical studies of the water breakdown process. The external circuit was included via a 50-Ω external resistor and a time-dependent supply voltage $V_{app}(t)$. A uniform mesh was used to divide the entire device-simulation region into equal-sized boxes. Transport was characterized on the basis of the drift-diffusion (DD) theory. The DD approach was used to update both the negative- and positive-ion densities within each box, taking account of inflows and outflows, bulk recombination and generation, charge creation due to field emission and impact ionization within microbubbles, negative-ion generation at the cathode due to electron tunneling into the liquid,

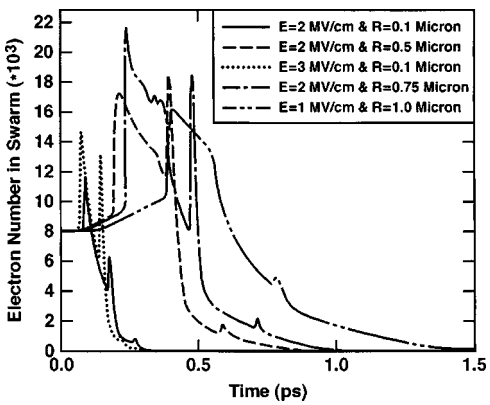

FIG. 7. Monte Carlo results for the time-dependent swarm starting with an initial 8000-particle population.

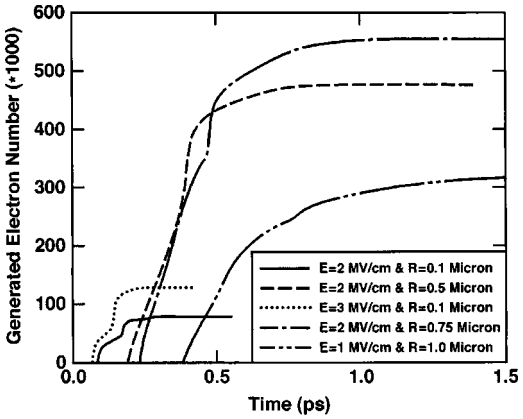

FIG. 9. Monte Carlo results showing secondary particle production outside a bubble as a function of time due to an 8000-particle swarm.

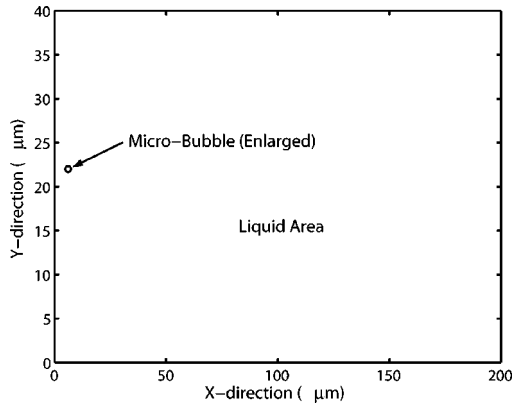

FIG. 10. Geometry and micro-bubble placement for the time-dependent breakdown simulation.

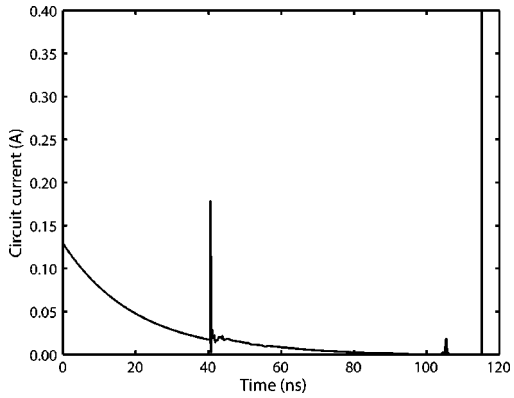

FIG. 11. Predicted time-dependent current for the geometry of Fig. 10.

positive-ion decay at the anode due to electron capture via the tunneling process, and positive-ion annihilation at the cathode via electron transfer. Monte Carlo results were incorporated to yield the microscopic generation rates and spatial distributions. The liquid was assumed to be free of impurities and to contain only the H^+ and OH^- ions. The ionic mobilities, taken from Light and Licht,[40] were 3.5×10^{-7} $m^2\,V^{-1}\,s^{-1}$ for H^+ and 2×10^{-7} $m^2\,V^{-1}\,s^{-1}$ for OH^-. Free electrons generated within the microbubble were considered and assigned a field-dependent drift velocity $v(F)$ given by $v(F)=v_s\{F/[F+F_s]\}$, with F as the electric field, v_s is the saturation velocity taken to be 3×10^5 m/s, and $F_s=3\times10^5$ V/m. Free electrons in liquid water were taken to have a lifetime of 200 ns. Current continuity was used to update the internal electric field $F(x,t)$ and the potential at grid points within the center of each box, through the relation $J_{cct}(t)=[V_{app}(t)-V_{Dev}(t)]/R=(d[\varepsilon(F)F(x,t)]/dt)+\sigma F(x,t)$, with V_{Dev} being the device voltage and $\varepsilon(F)$ the field-dependent permittivity.

An effective field-dependent permittivity was used based on a detailed atomic-level analysis of the electrical response of water dipoles at the metal-liquid interface.[35] This effectively leads to electric-field enhancements arising from a positive feedback mechanism, since permittivity decreases with increasing electric field. The cross sections were assumed to be rectangular, with a 200-μm distance between the point and plane electrodes, in keeping with the experimental setup within our group. The impact ionization process was modeled in terms of the spatial multiplicative gain factor $GF(r,t)$ taken from the Monte Carlo simulations, as discussed in Figs. 8 and 9. The rate of electron (and ion) production dn/dt was proportional to the field-dependent emission rate $G\{F(t-m\Delta t)\}$ at the bubble-liquid interface from all previous applicable time steps. Thus, the cumulative effect was included and time-delays in charge production from various locations downstream from the bubble were taken into account.

Time-dependent results for a rectangular simulation region shown in Fig. 10 with the anode at $x=0$ and the cathode on the opposite side are discussed next. The gap length was 200 μm, in keeping with experiments. The longitudinal axis of symmetry corresponds to $y=0$. For computational simplicity, the transverse dimension (along y axis) was restricted to 40 μm. Effectively then, only a small rectangular region close to the central axis was considered for these breakdown simulations. Figure 10 also shows a 0.5-μm-radius microbubble placed off-axis near the anode side. An open-ended 40-kV voltage pulse $[=V_{app}(t)]$ with an exponential rise time of 30 ns was chosen, in keeping with reported experimental voltage shapes. Since the focus here is on the breakdown initiation phase, the pulse turn-off characteristics were not considered. The time-dependent current obtained from the numerical simulation is shown in Fig. 11. The initial displacement current is apparent, followed by a small current spike after about 41 ns, and an eventual breakdown at ~116 ns. This breakdown delay time is in good agreement with actual experimental values. Snapshots of the internal voltage distribution at various times are given in Figs. 12(a)–12(c). Perturbations in the potential are seen to initiate from the microbubble location. Field emission at the bubble-water interface, followed by impact ionization of the gas, leads to rapid charge creation. The electric field between the microbubble and anode then decreases, while slow-moving ions drifting towards the cathode contribute to local field enhancement downstream. A streamer is seen to develop, and the voltage distribution moves in a narrow stripe towards the cathode. Charge is continually created at the tip as it advances through the field-emission process. Snapshots of the positive-ion density at 56.58 and 115.2 ns are shown in Figs. 13(a) and 13(b), while the electric field at 115.2 ns is given in Fig. 14. The field is seen to be highest at the tip of the advancing streamer. Eventually, just prior to the final breakdown, strong electron emission is predicted to initiate from the cathode. Beyond this time, for a short duration, there are two streamers (not shown) that move towards each other at a rapid rate. A snapshot of the electron density at 115.2 ns is given in Fig. 15. The sudden injection of electrons from the cathode side is evident in Fig. 15.

Next, simulations were also carried out for the same 200-μm configuration, but *without a microbubble*. The time-dependent current result is shown in Fig. 16, and no breakdown is predicted. This underscores the important influence of microbubbles in *initiating* liquid breakdown. Finally, simulations were carried out with three microbubbles placed in the simulation region. The additional bubble was placed roughly midway between the electrodes, as shown in Fig. 17. Results for the time-dependent current are given in Fig. 18.

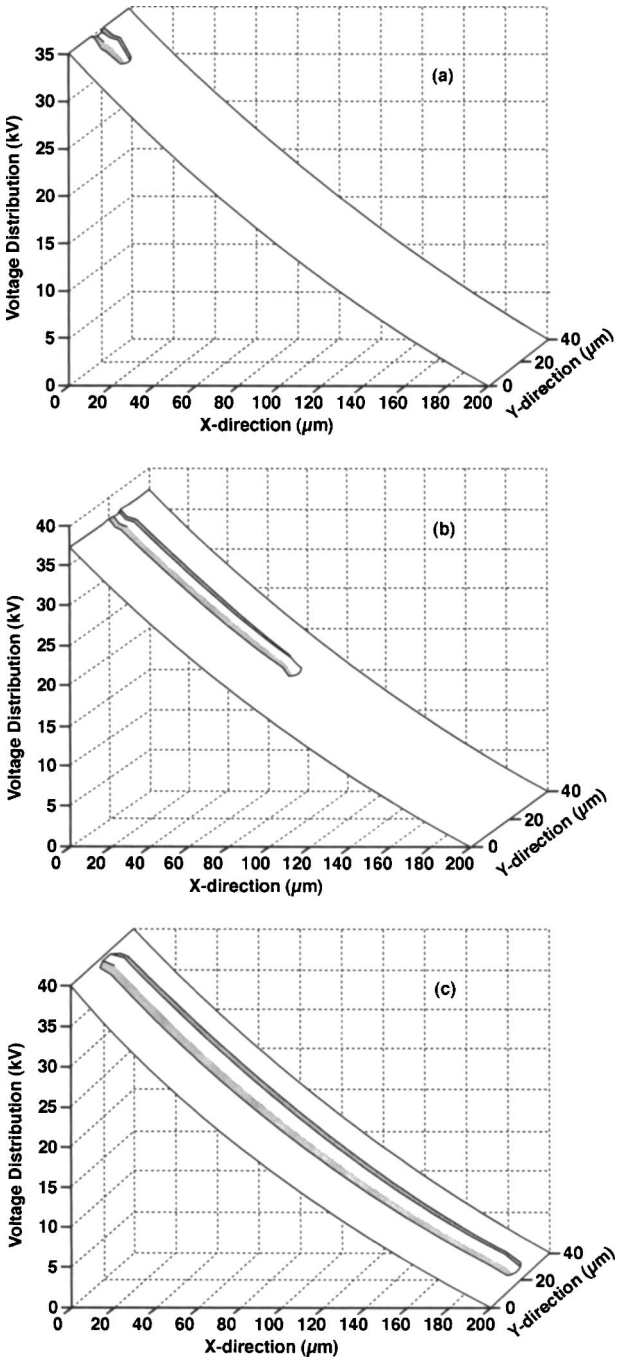

FIG. 12. Snapshots of the internal potential distribution at various times. (a) At 43.28, (b) 56.58, and (c) 115.2 ns.

In comparison to Fig. 11, the breakdown delay time is seen to be slightly smaller. This is expected, as the second microbubble provides additional contributions to charge generation and plasma generation within the liquid. Perturbations in the potential distribution (not shown), similar to the results of Fig. 12, were predicted to start from the region surrounding the microbubble closest to the anode. Figure 19 shows the positive-ion density at 88.1 ns. It clearly reveals the development of secondary branches. This behavior is similar to the experimental observations. This result demonstrates that such dendritic formations must be stochastic events that depend on both the local electric field and fluctuations in material density.

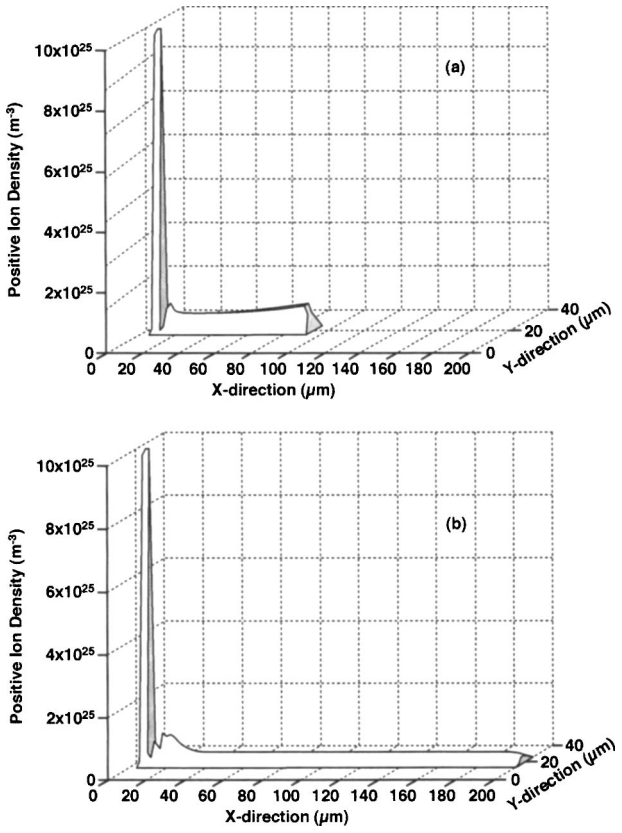

FIG. 13. Snapshots of the positive-ion distribution at times of (a) 56.58 and (b) 115.2 ns.

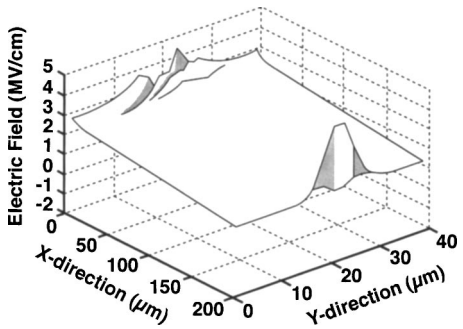

FIG. 14. Snapshot of the internal electric-field profile at 115.2 ns.

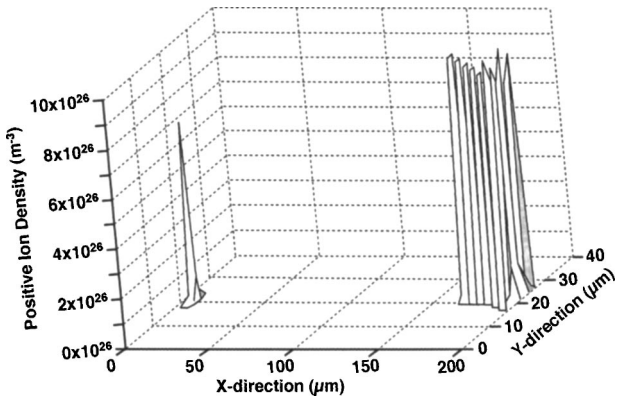

FIG. 15. Snapshot of the electron-density distribution just prior to breakdown.

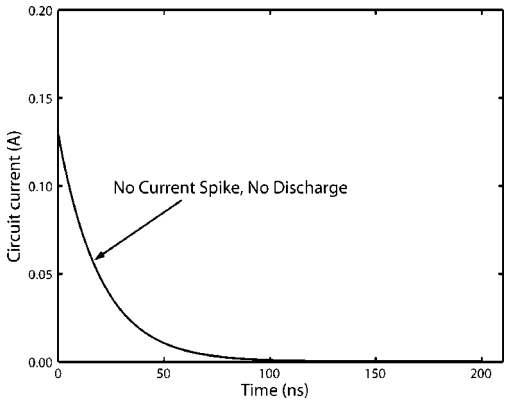

FIG. 16. The predicted time-dependent current for the same geometric configuration of Fig. 10, but without a microbubble.

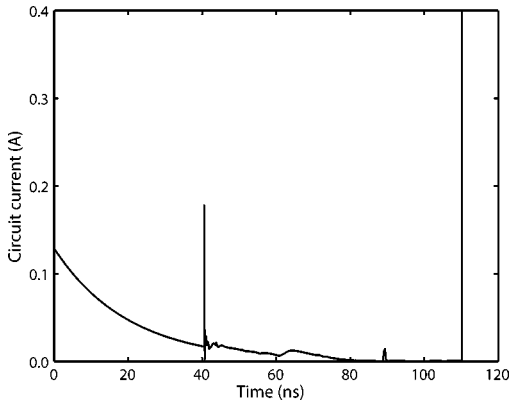

FIG. 18. The predicted time-dependent current for the geometry of Fig. 17.

V. SUMMARY AND CONCLUSIONS

In conclusion, we have analyzed the initiation physics of the electric breakdown process in liquid water for a short electrical pulse in the 100-ns range. The breakdown process has been probed on the basis of nonlinear, field-dependent mechanisms. It was shown that under low-density situations, electron-field emission followed by impact ionization would be operative. This makes for the creation of internal plasma microsources. Apart from pre-existing microbubbles, the use of external photoexcitation should similarly trigger breakdown.

A drift-diffusion model was used in this study to probe the time-dependent dynamics of breakdown. It was shown that the breakdown for a 200-μm water gap would roughly occur around 115 ns, triggered by a microbubble. The simulations clearly demonstrated streamer growth and movement towards the cathode. Radiative recombination and Bremsstrahlung associated with electrons and positive ions within the streamer column would conceivably produce the illumination observed during such breakdown. Furthermore, it was shown that branching of streamers and the formation of random dendritic structures could occur in the presence of an inhomogeneous distribution of microbubbles. The time-dependent current was shown to exhibit slight fluctuations as the microbubbles were successfully triggered internally. The simulations were also indicative of a time-dependent streamer velocity and dendritic growths from both electrodes, in keeping with recent experimental reports. The eventual cathode-side breakdown and electron emission were the result of a continuous increase in local electric field with streamer movement. This is a general process, and hence it would appear that electron emission from the cathode would eventually be established irrespective of the work function of the electrode material. Detailed modeling comparisons of the polarity effect will be presented elsewhere.

The present model also predicts that electrode smoothness would work to hold off the breakdown triggering by curtailing localized field enhancements. Similarly, it follows that lasers and optical pulses should help initiate breakdown and lower the hold-off voltage through photon-assisted, field emission. In such cases, electrons would not need as large an electric field to tunnel out, since photoabsorption would effectively reduce the energy barrier. Also, if all other parameters are made equal, then lower dielectric liquids would appear to present a better hold-off voltage capability, since the electric field within the microbubbles would be somewhat smaller. Other possibilities for increasing the hold-off voltage appear to be the use of surfactants to alter the surface tension for reducing microbubble sizes. Similarly, the addition of low-mobility ions that could screen out and mitigate electric-field penetration into microbubbles would help bolster the hold-off capability.

The high-field physics in liquids appears to be similar to that occurring in ceramics and nanogranular dielectrics. In

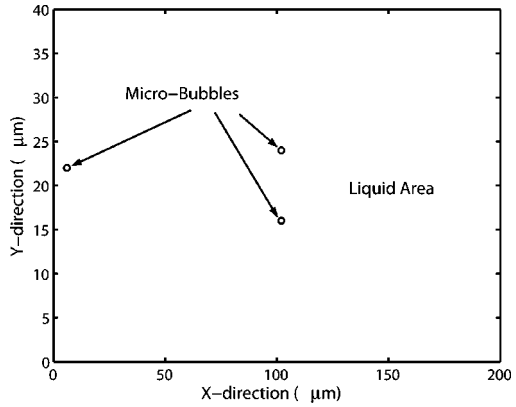

FIG. 17. A second geometry and microbubble placement for the time-dependent breakdown simulation.

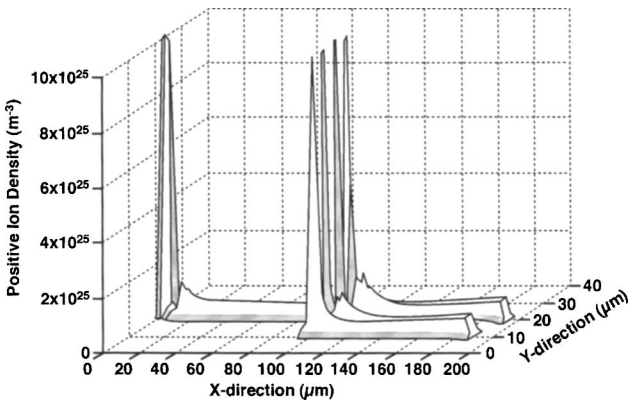

FIG. 19. Snapshot of the positive-ion density at 88.1 ns.

the latter case, strong electric fields at grain boundaries and associated microcavities trigger breakdown. As with nanogranular ceramics, charge trapping and its attachment to neutral molecules are likely to reduce the long-term hold-off capability in liquids. This would likely manifest itself as an aging-related degradation phenomenon. However, unlike ceramics and solids, it should be possible to flush out the liquid system via forced nonturbulent flow to curtail such detrimental degradations to an extent.

ACKNOWLEDGMENTS

This work was sponsored by an AFOSR-MURI grant (Grant No. F49620-01-1-0354) on Compact, Portable Pulsed Power (program manager, Dr. Robert J. Barker), and by Sandia National Laboratories. One of us (R.P.J.) appreciates useful discussions with J. Woodworth and J. Lehr (Sandia National Laboratories).

[1]H. Akiyama, IEEE Trans. Dielectr. Electr. Insul. **7**, 646 (2000).
[2]J. Gaudet *et al.*, Proc. IEEE **92**, 1144 (2004).
[3]J. Talati, T. Shah, A. Memon, M. Sidhwa, S. Adil, and A. Omair, J. Urol. (Baltimore) **146**, 1482 (1991).
[4]A. H. Olson and S. P. Sutton, J. Acoust. Soc. Am. **94**, 2226 (1993).
[5]M. Zahn, Y. Ohki, D. B. Fenneman, R. J. Gripshover, and V. Gehman, Jr., Proc. IEEE **74**, 1182 (1986).
[6]M. R. Patel, M. A. Barrufet, P. T. Eubank, and D. D. DiBitonto, J. Appl. Phys. **66**, 4104 (1989).
[7]I. Vitkovitsky, *High Power Switching* (Van Nostrand Reinhold, New York, 1987), pp. 116–137.
[8]D. L. Johnson, J. P. Vandevender, and T. H. Martin, IEEE Trans. Plasma Sci. **8**, 204 (1980).
[9]R. P. Joshi, J. Qian, and K. H. Schoenbach, J. Appl. Phys. **92**, 6245 (2002).
[10]S. Xiao, J. Kolb, S. Kono, S. Katsuki, R. P. Joshi, M. Laroussi, and K. H. Schoenbach, IEEE Trans. Dielectr. Electr. Insul. **11**, 604 (2004).
[11]P. K. Watson and A. H. Sharbaugh, J. Electrochem. Soc. **107**, 516 (1960).
[12]N. J. Felici, J. Electrost. **12**, 165 (1982); IEEE Trans. Electr. Insul. **20**, 233 (1985).
[13]A. Nikuradse, *Das Flηssige Dielektrikum* (Springer, Berlin, 1934), pp. 134–152.
[14]F. Pontiga and A. Castellanos, IEEE Trans. Dielectr. Electr. Insul. **3**, 792 (1996).
[15]E. E. Kunhardt, Phys. Rev. B **44**, 4235 (1991); H. M. Jones and E. E. Kunhardt, J. Appl. Phys. **77**, 795 (1995).
[16]E. O. Forster, IEEE Trans. Electr. Insul. **25**, 45 (1990).
[17]T. J. Lewis, IEEE Trans. Electr. Insul. **20**, 123 (1985).
[18]P. Keith Watson, W. G. Chadband, and M. Sadeghzadeh-Araghi, IEEE Trans. Electr. Insul. **26**, 543 (1991).
[19]A. Beroual, C. Marteau, and R. Tobazeon, IEEE Trans. Electr. Insul. **23**, 955 (1988); T. Aka-Ngnui and A. Beroual, J. Phys. D **34**, 794 (2001).
[20]J. Qian, R. P. Joshi, K. H. Schoenbach, E. Schamiloglu, and C. Christodoulou, IEEE Trans. Plasma Sci. **30**, 1931 (2002).
[21]R. P. Joshi, J. Qian, G. Zhao, J. Kolb, K. H. Schoenbach, E. Schamiloglu, and J. Gaudet, J. Appl. Phys. **96**, 5129 (2004).
[22]J. P. Hernandez, Rev. Mod. Phys. **63**, 675 (1991).
[23]Y. Sakai, W. F. Schmidt, and A. G. Khrapak, IEEE Trans. Dielectr. Electr. Insul. **1**, 724 (1994).
[24]J. V. Coe, Int. Rev. Phys. Chem. **20**, 33 (2001).
[25]R. Laenen, T. Roth, and A. Laubereau, Phys. Rev. Lett. **85**, 50 (2000).
[26]H. M. Jones and E. E. Kunhardt, IEEE Trans. Dielectr. Electr. Insul. **1**, 1016 (1994).
[27]J. M. Lehr *et al.*, "Multi-Megavolt Water Breakdown Experiments," in Proceedings of the 13th IEEE Pulsed Power Conference, 2003, pp. 609–614.
[28]M. Butcher, A. Neuber, H. Krompholz, and J. Dickens, "Optical Diagnostics of Liquid Nitrogen Volume Pre-Breakdown Events," in Proceedings of the 14th IEEE Pulsed Power Conference, Dallas, TX, 2003, pp. 1029–1032.
[29]J. R. Woodworth *et al.*, IEEE Trans. Plasma Sci. **32**, 1778 (2004).
[30]R. P. Joshi, J. Qian, and K. H. Schoenbach, "Model Analysis of Breakdown in High-Voltage, Water-Based Switches," in Proceedings of the 14th IEEE Pulsed Power Conference, Dallas, TX, 2003, pp. 293–296.
[31]N. F. Bunkin and F. V. Bunkin, Sov. Phys. JETP **74**, 271 (1992).
[32]Ya. B. Zel'dovich, Zh. Eksp. Teor. Fiz. **12**, 525 (1942).
[33]For example, L. D. Landau and E. M. Lifshitz, *Electrodynamics of Continuous Media* (Pergamon, Oxford, 1960).
[34]M. Arrayas, Am. J. Phys. **72**, 1283 (2004); M. Arrayas, U. Ebert, and W. Hundsdorfer, Phys. Rev. Lett. **88**, 174502 (2002).
[35]R. P. Joshi, J. Qian, K. H. Schoenbach, and E. Schamiloglu, J. Appl. Phys. **96**, 3617 (2004).
[36]C. Champion, Phys. Med. Biol. **48**, 2147 (2003).
[37]P. Teulet, J. P. Sarrette, and A. M. Gomes, J. Quant. Spectrosc. Radiat. Transf. **62**, 549 (1999).
[38]A. V. Phelps, Joint Institute for Laboratory Astrophysics Information Center Report No. 28, 1985 (unpublished).
[39]J. S. Morrill, W. M. Benesch, and K. G. Widing, J. Chem. Phys. **94**, 262 (1991).
[40]T. S. Light and S. L. Licht, Anal. Chem. **59**, 2327 (1987).